OPTOELECTRONICS AND ADVANCED MATERIALS – RAPID COMMUNICATIONS Vol. 3, No. 8, August 2009, p. 763 - 770

Electrical transport properties of n-type GaN

M. ARI*, H. METIN[a], Y. DAGDEMIR
University of Erciyes, Department of Physics, Kayseri, Turkey
[a]University of Mersin, Department of Physics, Mersin, Turkey

A theoretical model of energy loss mechanism as a function of electron temperature and electron concentration has been given forn-type GaN structures. The energy relaxation rates and mobility for warm and hot electrons have been calculated for over the electron temperature(T_e) range of 1.5 to 500 K at lattice temperature T_o=1.5 K. It has been found that the acoustic phonon scattering due to deformation potential and piezoelectric coupling are the dominant scattering mechanisms at low electron temperatures (T_e<100 K). For T_e >100 K, the polar optic phonon scattering becomes the effective scattering mechanism. The optic phonon energy of GaN was obtained as 91.8 meV and the PO phonon emission time as 8.6 fs. Also, the drift velocity of electrons as function of electron temperature and electric field has been obtained. The theoretical results are compared with available experimental results and a good agreement is observed.

(Received May 29, 2009; accepted July 20, 2009)

Keywords: Gallium nitride, Theory of electron transport, Mobility, Electron-phonon interaction

1. Introduction

Over the past decade, there has been a great deal of interest in the study of the transport properties of nitride-based material systems, such as GaN, due to their wide band gap [1-8]. Advantages associated with a large band gap include higher breakdown voltages, the ability to sustain large electric fields, lower generation noise, radiation hardness and high temperature operations. The nitride-based materials have also opened the opportunity to be used as emitters, detectors and microwave electronic devices. The nitride material systems have been shown to be very suitable for applications such as laser and light emitting diodes [9], ultraviolet detectors [10] and Bragg reflector [11]. For example, blue and violet laser emissions at room temperature have already been commercialized [12-14]. In addition, GaN based lasers are important for high density optical read-write technologies [12].

In order to analyse and improve the performances of devices based on these materials, an understanding of electron transport is necessary. The process of carrier energy relaxation is central to the behaviour of semiconductor devices. Investigating of carrier energy relaxation also give information about the electron-phonon interactions which are of fundamental importance in the physics of semiconductors. For these reasons, the energy relaxation mechanisms and the scattering processes have been extensively studied in III-V material based devices [15-24]. The scattering theories of the III-V materials have been developed by several workers [15, 16, 20-23, 25-27]. Though much progress has been made in developing GaN based devices, many problems still persist including surface breakdown, large gate leakage currents etc. Investigating the energy relaxation mechanisms of carriers in this material may help to understand and solve these problems. The main characteristics of the carrier-phonon interaction and the carrier energy dissipation in GaN are expected to be rather different to the relatively well understood GaAs. The reasons for this property are that, the large polar optic phonon energy in GaN, the strong piezoelectric constant at very low temperature, the strong impurity and defect scattering which can influence the electron-phonon interaction.

The main objective of this work is to investigate the electrical transport properties of n-type GaN structures. Firstly, the energy loss rates and mobility (μ) of electrons as a function of electron temperature (T_e) and electron concentration (n_e) have been determined by taking various scattering mechanisms such as the acoustic phonon scattering via deformation potential(DP), piezoelectric(PZ) coupling and the polar optic(PO) phonon scattering. Secondly, the GaN optic phonon energy and the PO phonon emission time τ were determined. Finally, electric field (E) and T_e dependence of drift velocity (v_d) of electron have been obtained.

2. Theoretical background

The electron-phonon scattering rate and their dependence of T_e and E can be used in order to determine the energy loss of an electronic system which gains energy from electric field and should transfer this energy to the lattice through collisions. As a results, the average energy on electron temperature of the electrons increases with the consequent decrease in the momentum relaxation time. Under steady state conditions, warm and hot electron phenomena are governed by the balance between the power input to the electronic system from the applied electric field and the energy loss of electrons, which are usually dominated by the inelastic collisions between the electrons and the phonons. It is possible that the fraction of excess energy leading to the heating of electrons can be known by using the power supply to the electronic system.

The joule input power per electron should be to be equated to the energy loss rate of electrons. So, the energy loss of electrons can be taken equal to the energy loss rate of phonons. By using balance equations, the energy loss rates and mobility of electrons as a function of T_e and n_e can be determined.

In order to investigate the contribution of energy dissipation of electrons via phonon scattering, the energy relaxation rates have to be calculated. In the materials of interest, the interaction of electrons and phonons may be treated by perturbation theory. The theoretically calculated energy loss rates differ from each other depending on the theoretical models adopted in their calculations. In order to test the various theoretical predictions about the behaviour of energy loss processes of the carriers due to different type of scattering mechanisms, one has to know which type of scattering is predominant in a given sample of material, temperature, carrier concentration and electric field range.

In this paper, we present a theoretical model for the energy relaxation rates and mobility from available theoretical approach. The theoretical calculations have been carried out by using the model given by Shah [23], Conwell [25], Seeger [26] and Lee et al. [27]. We have performed analytical electron temperature based model by using a weak perturbation based method. The energy relaxation rates and mobility expressions are given as a function of electron concentration and electron temperature. This allows us to determine T_e dependence of mobility and the energy loss rates of GaN for different electron concentrations. To obtain the energy relaxation rates of electrons, $\langle d\varepsilon/dt \rangle$, and the mobility μ, momentum and energy balance equations are used and can be given as,

$$\frac{1}{\mu} = \sum_j \frac{1}{\mu_j} \tag{1}$$

and

$$\sum_i \left\langle \frac{d\varepsilon}{dt} \right\rangle_i = eE^2 \left(\sum_j \mu_j\right) \tag{2}$$

the expressions for the various mobility μ_j and energy loss rates $\langle d\varepsilon/dt \rangle_i$ can be given by considering different scattering mechanisms.

The experimental and theoretical calculations for the steady state energy loss are based on the fundamental assumption that the electron-electron (e-e) scattering results in the thermalisation of the electrons. Hence, a non-equilibrium electron gas can be presented by a statistical electron temperature, T_e. In order to obtain the average rate of energy loss for electrons, it is necessary to specify the distribution function. A distribution that has been found convenient to use in this connection is the drifted Maxwell-Boltzmann distribution for the non-degenerate case. A method of calculating T_e dependence of energy loss of electrons with simplifying of a Maxwell-Boltzmann distribution consist of averaging momentum relaxation time over this distribution and calculating the energy loss rates as a function of T_e, from momentum and energy balance equations. The validity of this distribution, which depends on the dominance of the e–e scattering on the other scattering mechanism in thermalizing the electron distribution, is expected to hold even a high field due to the high electron concentration. Thus, we assume that the distribution function of the central valley electrons to be a drifted Maxwell-Boltzmann distribution.

In GaN, the presence of a strong internal polarization arising from the spontaneous and the PZ effects leads to the creation of stronger band bending and contributes to very high sheet carrier densities even in absence of intentional doping. Polarization arises in GaN due to its high ionicity which causes large PZ effects, hence PZ coefficients are almost in the order of magnitude larger than the traditional III-V materials [28]. This large PZ effect can also cause a large acoustic phonon scattering especially at low temperatures. Another acoustic phonon mode scattering mechanism is that due to the DP coupling. This mechanism is effective at low and intermediate temperatures. At high temperature, electrons lose their energies by emitting longitudinal optic phonon. Hence, the dominant scattering mechanism is the PO phonon scattering mechanism. In such cases, the main scattering mechanisms consist of scattering by the PZ acoustic phonon, the DP acoustic phonon and the PO phonon.

In the electron temperature approach, the energy relaxation rate can be given as a function of T_e and n_e. The expression for the energy loss rate term, $\langle d\varepsilon/dt \rangle$, as a function of T_e and n_e, can be defined by considering the different scattering processes. We expect that the energy flow from the electronic system will be mainly through the acoustic phonon emission via the DP and PZ coupling which dominant mechanisms of energy loss of GaN at low and intermediate temperature values.

If a crystal consists of dissimilar atoms such as GaN, the bonds are partly ionic and the unit cell does not contain a centre of symmetry and exhibiting strong PZ effects, especially at very low temperature, electron may be scattered by the acoustic phonons due to the PZ coupling. For the calculation of the energy loss rate as a function of T_e and n_e due to acoustic phonon via the PZ scattering for the non-degenerate case, the perturbation based model is used, as given by [23, 25-27,29],

$$\left\langle \frac{d\varepsilon}{dt} \right\rangle_{pz} = \frac{1}{n_e} \left(\frac{0.8m^3 (e_{14} e k_B T_e)^2}{\pi^3 \eta^5 \rho (\varepsilon_o \varepsilon_s)^2} \right) \left(1 - \frac{T_o}{T_e} \right) F_o(\eta) \tag{3}$$

and also mobility can be given by,

$$\mu_{pz} = \frac{1}{n_e} \left(\frac{8\rho k_B T_e^2}{1.2\pi e \eta T_o} \right) \left(\frac{u_l \varepsilon_o \varepsilon_s}{e_{14}} \right)^2 F_{1/2}(\eta) \tag{4}$$

here, k_B is the Boltzmann constant, ρ is the density of GaN, e is the electric charge of electron, m is the effective

mass of electron, T_o is the lattice temperature, u_l is the longitudinal sound velocity, e_{14} is piezoelectric constant, ε_s is the static dielectric constant of GaN, ε_o is the free space dielectric constant, η is the reduced Fermi energy and $F_j(\eta)$ are Fermi integrals.

Additionally, the scattering of conduction electrons by acoustic phonons requires the theorem of the deformation potential. The variation of conduction band edge with lattice constant can be taken linear for a small change in the lattice spacing as it occurs in an acoustic phonon. The change in the energy of electron is proportional to the periodic dilation in an acoustic phonon. The factor of proportionality is the deformation potential constant of the conduction band. In steady state, when all the acoustic modes are fully excited, the average energy loss per unit time of an electron to the crystal lattice due to acoustic phonon emission via the DP interaction at temperature T_e is given by,

$$\left\langle \frac{d\varepsilon}{dt} \right\rangle_{dp} = \frac{1}{n_e}\left(\frac{8D^2(k_BT_e)^3m^4}{\pi^3\eta^7\rho}\right)\left(1-\frac{T_o}{T_e}\right)F_1(\eta) \qquad (5)$$

and the mobility

$$\mu_{dp} = \frac{1}{n_e}\left(\frac{4e\rho u_l^2 T_e}{3\pi D^2 m\eta T_o}\right)F_1(\eta) \qquad (6)$$

where D is the DP constant.

At high electron temperature, the interaction of electrons with the optic phonons is known as the polar optic (PO) phonon scattering which becomes to dominate the energy relaxation mechanism. In the absence of hot phonon effects as assuming $T_e >> T_o$, the average energy loss rate per electron energy due to the PO phonon emissions is given by the expression[23, 25-27,29],

$$\left\langle \frac{d\varepsilon}{dt} \right\rangle_{po} = \frac{1}{n_e}\left(\left(\frac{(\eta\omega_o k_B T_e)^{3/2}(em)^2}{4\pi^3\eta^5\varepsilon_o}\right)\left(\frac{1}{\varepsilon_\infty}-\frac{1}{\varepsilon_s}\right)\right) \left(\frac{e^{X_o-X_e}-1}{e^{X_o}-1}X_e^{1/2}e^{X_e/2}\right)K_o\left(\frac{X_e}{2}\right)F_{1/2}(\eta) \qquad (7)$$

and mobility

$$\mu_{po} = \frac{1}{n_e}\left(\frac{3m(k_BT_e)^3}{2^{5/2}\pi E_o\eta^4\omega_o}\right)\left(\frac{e^{X_o}-1}{e^{X_e/2}}\right) \left[\left(e^{X_o-X_e}+1\right)K_1(X_e/2)+\left(e^{X_o-X_e}-1\right)K_o(X_e/2)\right]^{-1}F_{1/2}(\eta) \qquad (8)$$

here, $X_e = \eta\omega_o / k_BT_e$, $X_o = \eta\omega_o / k_BT_o$, ω_o is the PO phonon frequency for GaN. K_o and K_1 are the Modified Bessel Functions of the second kind. ε_∞ is the high frequency dielectric constant of GaN and E_o is the critical electric field strength. We assume here that the expressions for the energy loss rates as a function of T_e are the same form as those bulks GaN.

The theoretical results were obtained by numerical evaluation of equations (1-8).

3. Results and discussion

To test the validity of the theoretical model, the results of the calculated energy loss rate were compared with the experimental results of Stanton *et al* [24]. Also, the computed results of mobility have been compared with the experimental results of Nakamura *et al* [30]. Figure 1(a) and Figure 1(b) show the theoretical results of the energy loss rates per electron as a function of T_e in the range of $1.5<T_e<500$ K for the electron concentrations of 9.2×10^{24} m^{-3} and 1.13×10^{24} m^{-3}, respectively.

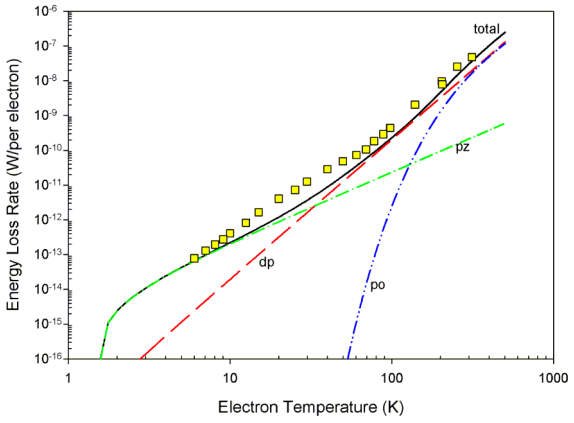

(a)

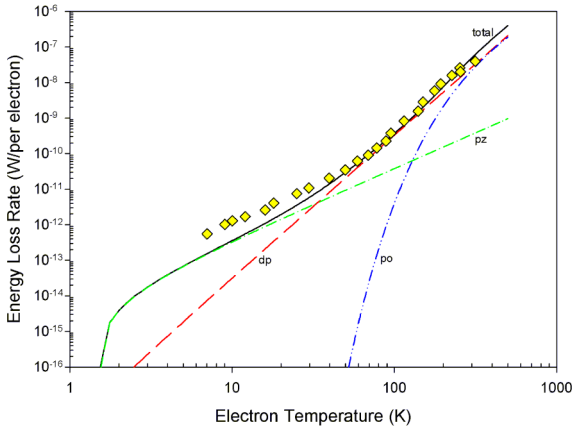

(b)

Fig. 1. The energy loss rates of electrons as a function of electron temperature in GaN at lattice temperature T_o=1.5 K. (a) for the electron concentration of 9.2 x10^{24} m^{-3} and (b) for the electron concentration of 1.13x10^{24} m^{-3}. The contributions of piezoelectric coupling (pz-dash_dot line), deformation potential (dp-dash line) and polar optic phonon emission (po-dash_dot_dot line) are shown by lines. The solid line shows the total contribution of the whole scattering mechanisms. The squares show the experimental results of Stanton et al [24].

Considering first the low and intermediate T_e region (T_e<100 K), the solid lines through the experimental data

points in Fig. 1 are obtained by numerical evaluation of eqs. (3, 5, 7). The calculated results confirm that the acoustic phonon scattering due to the PZ and DP interactions are dominant on the energy loss. As mentioned earlier, GaN materials exhibit strong PZ effects which is clearly seen in Fig.1 that the acoustic phonon scattering via the PZ coupling is higher than the acoustic phonon scattering due to the DP and the PO phonon scattering at very low electron temperatures T_e<35 K. In the temperature range of 35 K<T_e<100 K, the acoustic phonon scattering due to the DP interaction dominates the energy loss process.

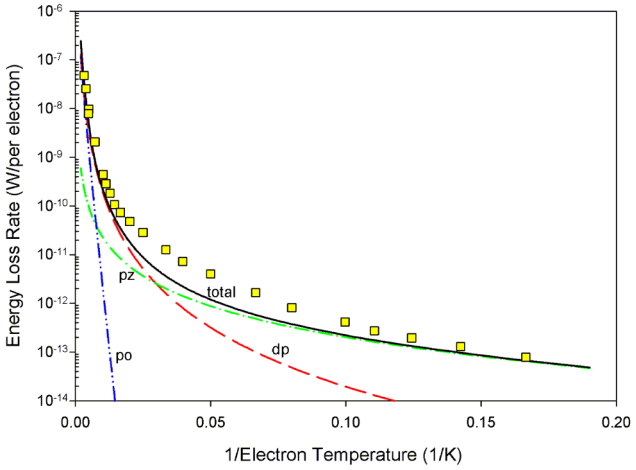

(a)

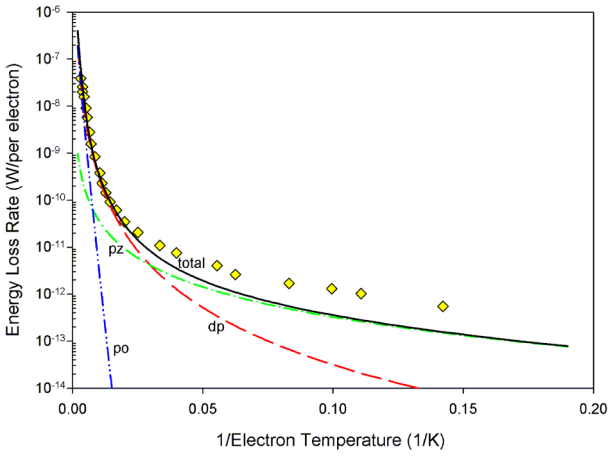

(b)

Fig. 2. The theoretical results for power loss per electron, P_e as a function of inverse electron temperature, $1/T_e$ (lines). (a) for n_e=9.2×10^{24} m^{-3}, (b) for n_e=1.13×10^{24} m^{-3}. The experimental results are also shown (squares).

Fig. 2 (a) and (b) show the energy loss rates per electron as a function of inverse T_e for two different n_e as the same of Fig. 1. Fig. 2 shows that the energy loss per electron is seen to increase with the increasing T_e. It is also clearly shown that the acoustic phonon mode scattering due to the PZ and DP coupling determines the energy loss processes in the electron temperature range of 1.5<T_e<100 K, which can be called the acoustic phonon region. The theoretical results of energy loss rates were compared with the experimental results of Stanton *et al* [24]. It can be seen from Fig.1 and Fig.2 that a good agreement is observed between the both results. A transition from the acoustic phonon emission due to the PZ coupling to the acoustic phonon emission due to the DP interaction occurs at the electron temperature $T_e \approx 35$ K. Therefore, the emission of the PZ coupled phonons is dominant at T_e<35 K. This situation is different to bulk GaAs for which the PZ coupling is much smaller**,** the DP coupling dominates the overall energy loss rate at all but the very lowest T_e [31]. The theoretical model is well able to account for the important features of the experimental results at low and intermediate electron temperatures. Therefore, it is possible to say that, the theoretical model works well in the acoustic phonon regime. However, it is also observed that at the acoustic phonon region, there is a region close to the PZ-DP coupling transition region where the experimental energy loss rates are larger than the theoretical value. This transition region can be seen from Figs. 1 and 2. Possible reason for this might be due to the screening effect of large piezoelectric coupling. This effect is not included in the theory of this study.

When T_e increases further, the PO phonon mechanism affects the energy relaxation processes. For T_e>100 K, the dominancy of the PO phonon scatterings can be seen in Fig.1 and Fig 2. Although, the acoustic phonon emission due to the DP coupling still exists, the contribution from the PZ coupling is much smaller than the other two scattering mechanisms. The agreement between the theoretical and experimental results of energy loss rates is also very good in this region.

A plot of ln(P_e) versus 1/T_e, gives a straight line at T_e>100 K in Fig. 2, where can be called optic phonon regime. From the slope of the line, the GaN optic phonon energy can be obtained as 91.8 meV, in good agreement with other methods [24, 32, 33]. The line intercepts the power loss axis at 1.7×10^{-5} W per electron, from $\langle d\varepsilon/dt \rangle = \eta\omega_o / \tau$, the PO phonon emission time τ was obtained as 8.6 fs. This value is also in good agreement with the theoretical value of 8.4 fs of the other model [24]. It is also clear from Fig.1 and Fig.2 that the theoretical model works also well at high temperature region. Therefore, the theoretical model used here works well to be able to account for the important features of energy loss mechanisms of GaN structure.

To test the validity of the theoretical model over an electron temperature range, we also calculate the mobility (μ) of electron for an electron concentration. The calculated results of μ compare with experimental mobility measurement of Nakamura *et al* [30]. Fig. 3 shows T_e dependence of mobility for n_e=3×10^{24} m^{-3}. As can be seen in Fig. 3 that, at T_e<90 K, the mobility increases with the increasing T_e, where the acoustic mode scattering dominates the transport process. Fig. 3 also shows that, the agreement between the computed results and the experimental results is good within the experimental uncertainty, especially at T_e<150 K. At T_e>150 K, the

theoretical results deviate from the experimental results. This implies that, there are other scattering mechanisms not included to the model that affect the mobility of electrons. Fig.3 shows that there is a region close to the acoustic-optic phonon crossover where the theoretical results of mobility deviate from the experimental mobility values. There could be several possible reasons for this discrepancy.

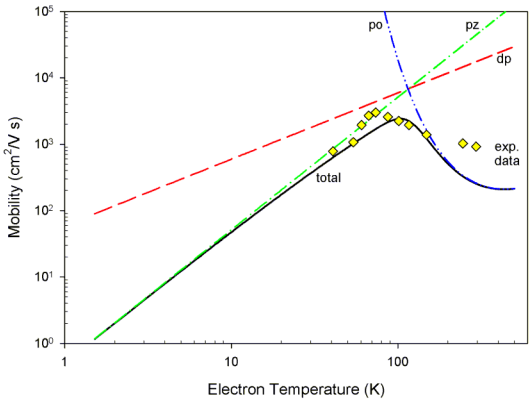

Fig. 3. Electron temperature dependence of electron mobility for the electron concentration of $n_e=3.0\times10^{24}$ m^{-3}. The solid lines are the theoretical results. The squares show the experimental results of Nakamura et al [30].

The samples might have the strong defect scattering and the momentum conservation selection rule relaxed. Also, the emission of coupled plasmon-optic phonon modes and emission of transverse optic phonons exist in the energy loss processes. Both the transverse optic phonon and plasmon-optic phonon coupling have a lower energy than the longitudinal optic phonons and so may be emitted at T_e below the crossover to longitudinal optic phonon emission. Therefore, the results in Fig.3 suggest that the emission of plasmon-optic phonon coupled modes leads to the increase of the energy relaxation rate.

It should be noted that, the model we have used in this study assumes that the momentum relaxation dependence on T_e is identical to its dependence on lattice temperature and also that n_e does not change with T_e. In the theoretical calculations, n_e is assumed to be constant for the whole T_e range. However, at high T_e, the electrons may be excited into non-conducting region. This observation might be directly related to the exponential decay of the current with electric field (E). The capture of electrons increases with the increasing E, hence mobility will gradually deviate further from the experimental results with the increasing T_e as observed. The hot electron capture may be associated with large potential fluctuations, which generally are seen in GaN [28].

Another reason of the discrepancy might be the presence of non-equilibrium hot phonons in the high temperature region. The behaviour of theoretically obtained results are gradually reduced with compared with experimental ones, what would be expected if there were hot phonons are present in this T_e region. However, the hot phonon reabsorption not only enhances the momentum relaxation rate but also reduces the energy relaxation rates. The more rapid increase in T_e with the increasing E is responsible for the reduction in mobility and thus in drift velocity due to the enhanced electron-phonon scattering. If this is correct, the magnitude of the experimental results should deviate from the theoretical results of the energy loss rate which does not include the hot phonon effect. In GaN materials, the electron-optic phonon interactions exist at high T_e region. Therefore, the hot phonon effect starts being effective mechanism and this may be one of the reasons for the discrepancy between theoretical and experimental results.

The other reason for the observed disagreement between the experimental and theoretical mobility results at high T_e, hence high E region, might be at variance with one of the other assumptions made in the theory. The model does not take into account the population of higher subbands which is more likely to occur in GaN and also ignores the possible surface charge effect on the electron transport. The other possible scattering mechanism is the intervalley scattering which is important at high temperature for bulk semiconductors, which is also not included to the theory. Therefore, the electronic system is no longer non-degenerate and the distribution of electrons should be described by different theoretical approach than the theory of this study.

In addition, the theoretical calculations for the steady state power dissipation are based on the fundamental assumption that the electron-electron (e-e) scattering results in the thermalisation of the electrons, and hence a non-equilibrium electron gas system can be represented by a statistical electron temperature. This assumption is true for an electron system that the energies lower than the optic phonon energy where the e-e interaction is strong enough to establish a maxwellian distribution. The e-e interaction is not taken into account in the theory. But, several workers [34, 35] indicate that one of the main scattering mechanism is the e-e scattering which determines the energy and momentum relaxation rate in the high T_e region. Therefore, the accuracy of the electron temperature model which we have used in this study to obtain mobility for higher T_e region is questionable.

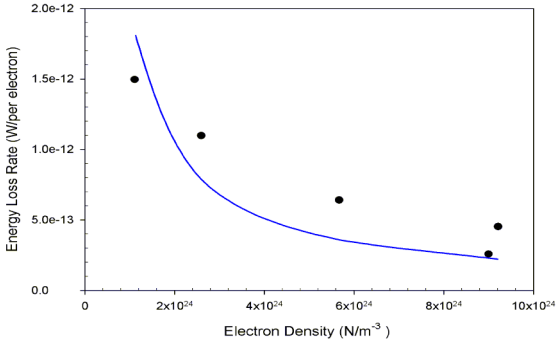

Fig. 4. Energy loss rates per electron at $T_e=10$ K and lattice temperature $T_o=1.5$ K as a function of the electron concentration. The solid line shows the results of theoretical calculation. The dots show the experimental results of Stanton et al [24].

The expressions which are used in this work, for the various energy loss rates and mobility terms are also dependent on n_e. This gives us the possibility to calculate the mobility and the energy loss rates as a function of n_e. Figure 4 shows the dependence of the energy loss rates on various n_e at T_e=10 K. The Figure clearly shows that, the energy loss rate is nearly independent of n_e at low T_e, where the PZ coupling is the dominant scattering mechanism. When the acoustic phonon emission due to the DP interaction and the optic phonon emission dominate the processes, the energy loss rate is seen to decrease with the increasing n_e. We compare the computed results with the experimental results of Stanton *et al* [24]. A reasonable good agreement is obtained between theory and experimental measurement within the experimental uncertainty. The solid line is obtained by numerical evaluation of eqs. (3, 5, 7).

We have also obtained T_e and E dependence of υ_d by using the equation of $\langle d\varepsilon/dt \rangle = eE\upsilon_d$ for n_e=9.2x10^{24} m^{-3}. The results are shown in Figs. 5 and 6. Fig. 5 shows that, υ_d increases linearly with the increasing E in the range of E<1 V/cm. Then, it starts to increase very sharply in the range of 1<E<10 V/cm which is the first part of the acoustic phonon scattering regime due to the deformation potential. Fig. 5 also shows that, when E >10 V/cm, υ_d starts to saturate at 2.5×10^6 cm/s, corresponds to the electric field region where the PO phonon scattering dominates both the momentum and the energy dissipation. Also, υd stay almost constant with E up to 2×10^3 V/cm in the same phonon regime.

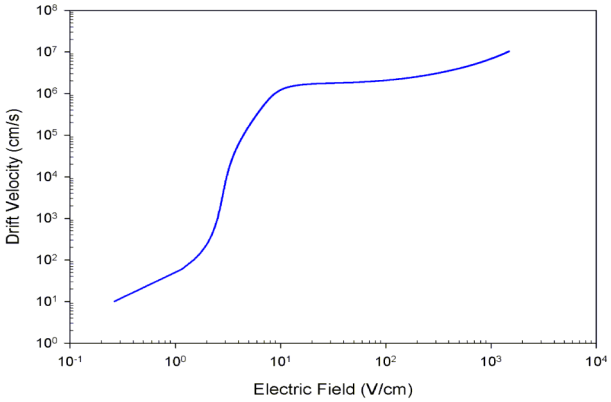

Fig. 5. Electric field dependence of drift velocity for the carrier concentration of n_e=9.2x10^{24} m^{-3} at the lattice temperature of T_o=1.5 K.

When the acoustic phonon emission via the PZ coupling dominates totally the energy loss processes, υ_d is increasing sharply with T_e at T_e<2 K, which can be seen from Fig. 6. Electron heating is seen to occur at T_e>2 K. The drift velocity increases linearly with T_e up to 100 K, after where it starts to saturate. At the first part of linear region, the PZ coupling determines the electron behaviour. Then, the DP interaction starts to involve to the process and stay effective up to the end of the region, in the range of 35 K<T_e<100 K. At the end of this region, the PO phonon scattering starts to influence the electron transport and electron becomes hot. The mobility of electronic system decreases with the increasing temperature.

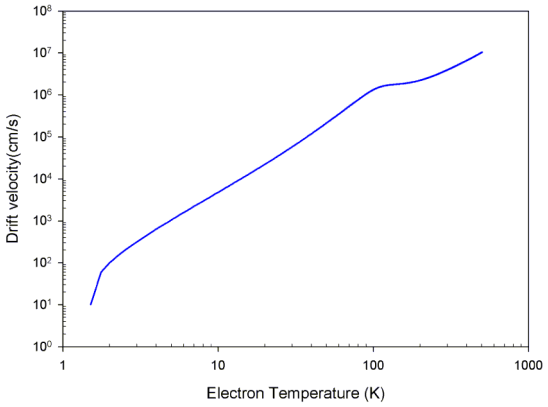

Fig. 6. Drift velocity of electrons as function of electron temperature for the electron concentration of n_e=9.2x10^{24} m^{-3} at the lattice temperature of T_o=1.5 K.

The electric field dependence of electron temperature is shown in Fig. 7. In the low temperature region, T_e almost not changes and stays constant with electric field (E<1 V/cm), where the energy loss rates have been determined by the acoustic phonon emission due to the PZ coupling. Then, the electron heating is starting at E>2 V/cm and T_e>2 K and T_e starts to increase very sharply with field in the electric field range of 2<E<10 V/cm up to T_e = 100 K, where the acoustic mode phonon scattering dominates the energy loss processes. Above this electric field range (E>10 V/cm), T_e increases more slowly with E, where the dominant energy loss mechanism is the PO phonon scattering. At this region, the electrons start to degenerate and hot phonons become effective.

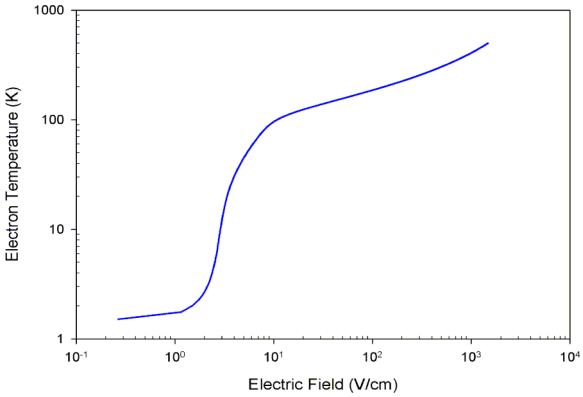

Fig. 7. Electric field dependence of electron temperature for the electron concentration of n_e=9.2x10^{24} m^{-3} at the lattice temperature of T_o=1.5 K.

From Figs. 5-7, we can concluded that, at very low fields (up to ~0.1 V/cm) where the all of the electrons reside in the lowest subband, υ_d increases linearly with E, with a mobility of ~100 cm^2/V s. This mobility low compared to the room temperature, which can be seen from Fig. 3. The low field mobility may be influenced by the electron-acoustic phonon interaction due to the PZ

coupling. Above this electric field region, the mobility of electrons is the highest value of ~3000 cm^2/V s in the range of $0.1<E<10$ V/cm. For the electric field above about 10 V/cm, the drift velocity saturates and the cool electrons become hot. The mobility of the electronic system starts to decrease at this electric field region. It is possible to say that, the velocity saturation effects and repopulation of the various subband energy levels play significant roles in the velocity-field curves.

4. Conclusions

In this study, the electron transport properties were examined through theoretical calculations of electron-phonon interaction effects. The variation of energy loss mechanisms and mobility of electrons with electron temperature and electron concentration have been investigated by using the weak perturbation based theory for n-type GaN. For the energy loss rates and mobility of electron calculations, the acoustic phonon scattering due to the deformation potential and the piezoelectric coupling and also the polar optic phonon emission mechanisms were taken into account. The results were obtained in the electron temperature range of 1.5 to 500 K at the lattice temperature of 1.5 K.

To test the theoretical model, the computed results of energy loss rates of electrons were compared with the experimental results of Stanton *et al* [24], for two different electron concentrations. The agreement between theoretical and experimental results is very good over all electron temperature. It can be clearly seen that, the main energy loss process is the acoustic phonon scattering at low electron temperatures $T_e<100$ K and the optic phonon emission at high electron temperature $T_e>100$ K.

Also, the mobility of electrons were calculated and compared with the experimental mobility measurement of Nakamura *et al* [30] and a good agreement has been obtained, especially in the electron temperature range of $T_e<150$ K. Above this temperature range, the results predicts that, other extra scattering mechanism should be included to the theory.

Acknowledgements

The author would like to acknowledge the support received for this work from the Erciyes University Research Fund (project no: FBA-07-041).

References

[1] Y. F. Wu, B. D. Keller, S. Keller, D. Kopolnek, P. Kozuday, S. D. Denbaars, U. K. Mishra, Appl. Phys. Lett. **69**, 1438 (1996).
[2] S. N. Mohammad, A. Salvador, H. Morkoç, Proc. IEEE **83** 1306 (1995).
[3] C. E. Martinez, N. M. Stanton, A. J. Kent, M. L. Williams, I. Harrison, H. Tang, J. B. Webb, J. A. Bardwell, Semicond. Sci. Technol. **19**, 440 (2004).
[4] R. P. Joshi, Appl. Phys. Lett., **64** 223 (1994).
[5] S. Nakamura, T. Mukai and M. Senoh, Appl. Phys. Lett. **64**, 1687 (1994).
[6] D. L. Smith, Solid State Commun. **57**, 919 (1986).
[7] S. Keller, G. Parish, P.T. Fini, S. Heikman, C.H. Chen, N. Zhang, S.P. DenBaars, U.K. Mishra, F. Wu, J. Appl. Phys. **85**, 5850 (1999).
[8] R. Gaska, M. Shur, A. D. Bykhovski, A. O. Orlov, G. L. Snider, Appl. Phys. Lett. **74**, 287 (1999).
[9] H. Morkoç, S. N. Mohammad, in Wiley Enclopedia of Electrical and Electronics Engineering, edited by J. Webster, John Wiley and Sons, New York, 1999.
[10] M. Razeghi, A. Rogalski, J. Appl. Phys. **79**, 7433 (1996).
[11] I. J. Fritz, T. J. Drummond, Electron. Lett. **31**, 68 (1995).
[12] T. Mukai, S. Nakamura, Jpn. J. Appl. Phys. **38**, 5735 (1999).
[13] G. E. Bulman, K. Doverspike, S. T. Sheppard, T. W. Weeks, H. S. Kong, H. M. Dieringer, J. A. Edmond, J. D. Brown, J. T. Swindell, J. F. Schetzina, Electron. Lett. **33**, 1556 (1997).
[14] S. Nakamura, M. Senoh, N. Iwasa, S. Nagahama, T. Yamada, T. Mukai, Jpn. J. Appl. Phys. **34**, L1332 (1995).
[15] B. K. Ridley, Rep. Prog. Phys. **54**, 169 (1991).
[16] P. J. Price Surf. Sci. **43**, 145 (1984).
[17] E. M. Daniels, B. K. Ridley, M. Emeny, Solid State Electron. **32**(12), 1207 (1989).
[18] K. Lee, S. Shur, T. J. Drummond, H. Morkoc, J. Appl. Phys. **54**, 6432 (1983).
[19] A. J. Cross, A. J. Kent, P. Hawker, D. Lehmann, Cz. Jasiukiewicz, M. Henini, Physica B **263-264**, 526 (1999).
[20] S. Gokden, N. Balkan, B. K. Ridley, Semicond Sci Technol. **18**, 206 (2003).
[21] J. Shah, Solid State Electron. **32**, 1051 (1989).
[22] R. Gupta, B. K. Ridley Solid State Electron. **32**, 1241 (1989).
[23] J. Shah, The Physics of The Two Dimensional Electron Gas, edited by J. T. Devreese, F. M. Peters, Plenum New York, NATO ASI Series b **157**, 183 (1987).
[24] N. M. Stanton, A. J. Kent, A. V. Akimov, P. Hawker, T. S. Cheng, T. J. Foxon, J. Appl. Phys. **89**, 973 (2001).
[25] E. M. Conwell , Solid State Physics, Supplement **9**, edited by F. Seitz, D. Turnbull and H. Ehrenreich, Academic, New York, 1967.
[26] K. Segeer, Semiconductor Physics: an introduction **7**. ed., Springer-Verlag, Berlin, 1999.
[27] H. P. Lee, D. Vakhshoori, Y. H. Lo, S. J. Wang, Appl. Phys. **57**, 4814 (1985).
[28] K. Kim, W. R. Lambrecht, B. Phys Rev B **53**, 6310 (1996).
[29] M. Ari, H. Metin, J. Optoelectron. Adv. Mater. – Rapid Comm. **5**, 2009 (accepted for publication).
[30] S. Nakamura, T. Mukai, M. Senoh, J. Appl. Phys **71**, 5543 (1992).

[31] M. Ari, M. Turkoglu, Physica B **337**, 199 (2003).
[32] Semiconductors: Basic data, 2nd edited by O. Madelung, Springer-Verlag, Berlin, 1996.
[33] Gallium Nitride and Related Semiconductors, edited by J. H. Edgar, S. Strite, I. Akasaki, H. Amano, C. Wetzel, INSPEC, London, 1999.
[34] N. Balkan, M. C. Arıkan, S. Gökden, V. Tilak, B. Schaff, R. J. Shealy, J Phys. Condens. Matter., **14**, 3457 (2002).
[35] Z. A. Zakhleniuk, B. K. Ridley, M. Babiker, C. R. Bennett, Physica B **272**, 309 (1999).

*Corresponding author: ari@erciyes.edu.tr